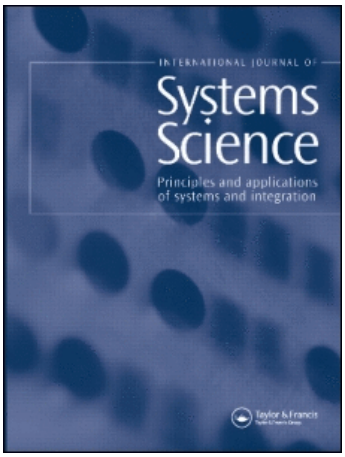

International Journal of Systems Science
Publication details, including instructions for authors and subscription information:
http://www.informaworld.com/smpp/title~content=t713697751

Generation of scale-free topology in complex networks by phase entrainment

I. Leyva [a]; I. Sendiña-Nadal [a]; J. M. Buldú [a]; J. A. Almendral [a]; S. Boccaletti [b]
[a] Complex Systems Group, Dep. Teoria de la Señaly Comunicaciones, Universidad Rey Juan Carlos, Móstoles, Madrid, Spain [b] CNR-Istituto dei Sistemi Complessi, Sesto Fiorentino, Florence, Italy

Online Publication Date: 01 September 2009

To cite this Article Leyva, I., Sendiña-Nadal, I., Buldú, J. M., Almendral, J. A. and Boccaletti, S.(2009)'Generation of scale-free topology in complex networks by phase entrainment',International Journal of Systems Science,40:9,923 — 930
To link to this Article: DOI: 10.1080/00207720802556278
URL: http://dx.doi.org/10.1080/00207720802556278

International Journal of Systems Science
Vol. 40, No. 9, September 2009, 923–930

Taylor & Francis
Taylor & Francis Group

Generation of scale-free topology in complex networks by phase entrainment

I. Leyva[a]*, I. Sendiña-Nadal[a], J.M. Buldú[a], J.A. Almendral[a] and S. Boccaletti[b]

[a]*Complex Systems Group, Dep. Teoria de la Señaly Comunicaciones, Universidad Rey Juan Carlos, Móstoles, Madrid, Spain;* [b]*CNR–Istituto dei Sistemi Complessi, Sesto Fiorentino, Florence, Italy*

(*Received 29 April 2008; final version received 8 October 2008*)

A collection of connected phase oscillators, initially unsynchronised, are subjected to a growing process. In such a process, pacemaker oscillators attach to the original network following an exclusively dynamical criterion oriented to entrain the network. Under these conditions, we show that successful entrainment always corresponds to the generation of a scale-free topology in the original graph.

Keywords: complex networks; scale-free; synchronisation; entrainment; coupled oscillators

1. Introduction

A great amount of natural and technological systems can be optimally modelled by a growing network of dynamical units (Boccaletti, Latora, Moreno, Chavez, and Hwang 2006b). The observation of these real networks reveals the reiterated presence of specific structural features, in particular the so-called scale-free property (Barabási and Albert 1999), consisting of the fact that the node connectivity degree k shows a power-law distribution $P(k) \sim k^{-\gamma}$. Additionally, it is known that the functionality and emerging properties of these complex ensembles is often connected to the total or partial synchronisation of the units in a collective dynamics, as the case of neurons in the neural tissue.

Then, a very relevant question is to understand how the intimate relationship between dynamics and structure can shape the network and generate the collective behaviours observed in it. Different aspects of how the topology influences the dynamics have been previously studied. Good examples are the attention concentrated to issues such as how the network structure can enhance synchronisation (Chavez, Hwang, Amann, Hentschel, and Boccaletti 2005a, b; Motter, Zhou, and Kurths 2005) or how proper topological mechanisms of network reshaping can improve or worsen the arousal of a synchronised behaviour (Yin, Wang, Chen, and Wang 2006), or even how a dynamical evolution of the topology eventually leads to stabilise a synchronous motion in cases in which static graph configurations would instead prevent synchronisation (Boccaletti et al. 2006a; Stilwell, Bollt, and Roberson 2006).

On the other hand, the reverse problem, i.e. how dynamics can drive the structure of a network, has not yet been fully addressed, and studies have been so far limited to the field of game theory (Ebel and Bornholdt 2002; Zimmermann, Eguíluz, and Miguel 2004), where it has been shown that a not growing network of players can be shaped by means of a decision game. We have recently approached the question in Ref. (Sendiña-Nadal, Buldú, Leyva, and Boccaletti 2008), where we demonstrated that dynamical criteria oriented to entrain an original set of networking oscillators are able to fully reshape the structure of the original graph, and that the entrainment process induces a scale-free degree distribution in the pristine network. This process can be considered as a representation of phenomena occurring in social science as the emergence of consensus driven by an opinion leader (media, press, fashion, publicity, etc.), or in biological systems as the entrainment of circadian clocks.

In the present work, we report a deeper insight on the interrelation mechanisms between topology and dynamics in a network of phase oscillators. In particular, we carefully study the time evolution of the topological changes along the growing process. The dependences on a wider range of parameters are also considered, obtaining a broader scope of the generality of the results. This article is organised as follows: in Section 2 we present the model, and study the dynamical conditions for which the growing process succeeds in entraining the network. In Section 3, we study the topological changes induced by the growth of the network, both in the synchronised and unsynchronised cases. Finally, in Section 4

*Corresponding author. Email: inmaculada.leyva@urjc.es

ISSN 0020–7721 print/ISSN 1464–5319 online

DOI: 10.1080/00207720802556278
http://www.informaworld.com

we present some discussion about the results and derive the relevant conclusions.

2. The model and numerical results

For the sake of exemplification, we here consider an initial ($t=0$) graph $\mathcal{G}_0$ of n_0 bi-directionally coupled Kuramoto phase oscillators (Kuramoto 1984), modelled by

$$\dot{\phi}_i = \omega_{0i} + \frac{d_0}{k_i(t=0)} \sum_{j=1}^{n_0} a_{ij} \sin(\phi_j - \phi_i)$$

where i runs from 1 to n_0, $k_i(t=0)$ is the initial number of incoming links to the i-th oscillator (known as the in-degree), and d_0 is a coupling constant. The natural frequencies of the phase oscillators $\{\omega_{0i}\}$ are uniformly distributed within the range $\bar{\omega}(t=0) = 0.5 \pm 0.25$. $\{a_{ij}\}$ are the $n_0 \times n_0$ elements of the adjacency matrix $\mathbf{A} = (a_{ij})$, describing the structure of the network of connections in $\mathcal{G}_0$, being $a_{ij}=1$ if there is a link from the oscillator j to i and $a_{ij}=0$ otherwise. Time integration is performed here by means of a Heun algorithm with an integration step $\Delta t_{in} = 0.1$.

Initially, we generate the original structure of $\mathcal{G}_0$ from a ring lattice of n_0 sites, each one bidirectionally linked to its $k_{0i} = 2m_0$ nearest neighbours. Then, links are randomly rewired with probability $p = \ln(n_0)/n_0$ (chosen to assure the generation of a giant connected component) to obtain a structure that exhibits the small-world property (i.e. the average shortest path length $L \propto \log\, n_0$ (Strogatz 2000)), and an exponentially decaying degree distribution $P_0(k)$ with a maximum around the mean value $\langle k \rangle = 2m_0$.

3. The growing process

Once the structure is defined, nodes in $\mathcal{G}_0$ are bidirectionally coupled with coupling strength d_0, which is selected so that the initial graph does not display a phase synchronised motion. Then, the pristine network is left to evolve in its unsynchronised motion from $t=0$ to $t=t_0=30$ time units. At this point, a growing process starts, consisting in a progressive adding of pacemaker oscillators on top of the $\mathcal{G}_0$. Specifically, at regular time intervals $t_l = t_0 + l\Delta t$, a pacemaker node is added to form m unidirectional connections with nodes on $\mathcal{G}_0$. The newly added nodes are identical phase oscillators that follow the instantaneous phase dynamics of an external pacemaker $\dot{\phi}_p = \omega_p$. New links are introduced unidirectionally to preserve the pacemaker character of the added nodes, and therefore they constitute a driving force for $\mathcal{G}_0$.

Notice that such a process is fully equivalent to consider a unique external driving node that forms successive (and possibly multiple) connections with nodes in $\mathcal{G}_0$ in the attempt to entrain their dynamics. Our choice, in terms of multiple identical pacemakers, allows us to compare the results with the vast majority of existing literature on graphs, since the other equivalent possibility would correspond to generate a multigraph in which a single node in $\mathcal{G}_0$ could be multiply connected to a single pacemaker.

The key point is how to fix the criterion through which the added nodes are linked to $\mathcal{G}_0$. We here consider a dynamical criterion fully oriented to enhance phase entrainment. When the l-th new node attaches to $\mathcal{G}_0$, it forms m connections preferentially with those nodes in $\mathcal{G}_0$ whose instantaneous phases at time t_l, $\phi_j(t_l)$, are closer to a given phase condition. Specifically, we consider a generic parameter $\delta \in (0, 2\pi)$ and establish the first of the m connections with that node j whose actual value of the phase fulfills the condition

$$\min_{j=1,\ldots,n_0} \left\{ |\delta - \Delta\theta_j| \bmod 2\pi \right\},$$

where

$$\Delta\theta_j = \phi_j(t_l) - \phi_p(t_l).$$

When $m > 1$, we repeat the above condition excluding those nodes that already received a link at the same time step. We initially set the value of this parameter as $m=1$.

Additionally, we will show that the specific choice of the parameter δ does not affect qualitatively the reported scenario. The only constrain is that δ cannot be taken equal to 0 nor to 2π, as these values correspond to the stable fixed point emerging during the phase locking of a single oscillator, and therefore these settings would determine a situation in which the first node of $\mathcal{G}_0$ that becomes entrained would attract the rest of the connections.

Each new connection is unidirectional, and it goes from the added node to the selected node in $\mathcal{G}_0$, having a coupling strength of d_p. The dynamics is now described by (Sendiña-Nadal et al. 2008)

$$\dot{\phi}_i = \omega_{0i} + \frac{d_0}{k_i(t)} \sum_{j=1}^{n_0} a_{ij} \sin(\phi_j - \phi_i) + \frac{d_p}{k_i(t)} \sum_{r=1}^{l(t)} b_{ir} \sin(\phi_p - \phi_i), \quad (1)$$

where $k_i(t)$ is the time evolving in-degree of the i-th node (which accounts for the new connections received from the added nodes), the matrix $\mathbf{B} = (b_{ir})$ is a size evolving matrix of $n_0 \times l(t)$ elements (with $l(t) \le n_1$,

being n_1 the total number of added pacemakers) whose entries b_{ir} are equal to 1 if there is a link from the r-th added node to the i-th node in $\mathcal{G}_0$ and zero otherwise.

Figure 1 reports the behaviour of several useful measures for quantifying the entrainment process. The panels (a) and (b) in Figure 1 show, respectively, the final $\mathcal{G}_0$ mean frequency $\langle\bar{\omega}(t)\rangle_t$ and its standard deviation $\langle\sigma_{\bar{\omega}}(t)\rangle_t$ *versus* d_p, for $n_0 = 1000$, $d_0 = 0.2$, $n_1 = 10{,}000$, $\Delta t = \Delta t_{in}$, and $\delta = \pi$ (anti-phase coupling condition), and three values of the entrainment frequency, where $\langle\ldots\rangle_t$ denotes an average over time (performed after the growing process is finished). Here $\bar{\omega}(t) = \frac{1}{n_0}\sum_{i=1}^{n_0}\dot{\phi}_i(t)$ is the ensemble average frequency at each time step, with a standard deviation given by

$$\sigma_{\bar{\omega}}(t) = \sqrt{\frac{1}{n_0}\sum_{i=1}^{n_0}\left[\dot{\phi}_i(t) - \bar{\omega}(t)\right]^2}.$$

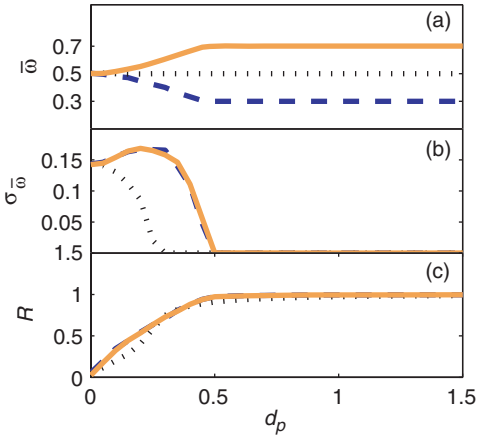

Figure 1. Time averaged phase synchronisation parameters (a) $\bar{\omega} = \langle\bar{\omega}(t)\rangle_t$, (b) $\sigma_{\bar{\omega}} = \langle\sigma_{\bar{\omega}}(t)\rangle_t$ and (c) $R = \langle R(t)\rangle_t$, as a function of the coupling strength d_p, for a network with $n_0 = 1000$, $n_1 = 10{,}000$, $\delta = \pi$, and three values of the entrainment frequency: $\omega_p = 0.7$ (orange-solid line), $\omega_p = 0.5$ (black-dotted line) and $\omega_p = 0.3$ (blue-dashed line). Each point is an average over 10 different realisations of the growing process.

It can be seen that the final state corresponds to full synchronisation to the pacemaker frequency. In Figure 1(c) we show the value of $R = \langle R(t)\rangle_t$ *versus* d_p, where $R(t)$ stands for the phase synchronisation order parameter (Kuramoto 1984)

$$R(t) = \frac{1}{n_0}\left|\sum_{j=1}^{n_0} e^{i\phi_j(t)}\right|.$$

From Figure 1(b) it is evident that the threshold for the setting of the phase entrainment of $\mathcal{G}_0$ ($R \simeq 1$) depends on the frequency of the external pacemaker ω_p. Specifically, as far as ω_p is close to $\bar{\omega} = 0.5$ (the initial average frequency of the oscillators in $\mathcal{G}_0$), the phase entrainment process occurs already for a relatively small value of d_p. On the contrary, when ω_p deviates significantly from $\bar{\omega}$, the value of d_p producing phase entrainment becomes larger and larger.

A more quantitative description of the entrainment process can be gathered by inspection of Figure 2. There, we report the time evolution of the mean frequency of the oscillators in the ensemble $\mathcal{G}_0$, $\bar{\omega}(t)$, its frequency dispersion $\sigma_{\bar{\omega}}(t)$ and $R(t)$, for three pacemaker frequencies ($\omega_p = 0.3$, 0.5 and 0.7) and three different pacemaker coupling strengths ($d_p = 0.2$, 0.5 and 1.5). It is seen that, while the low coupling regime is not associated to a phase entrainment of $\mathcal{G}_0$ with the pacemaker, in the high coupling regime $\bar{\omega}(t)$ converges (after the growing process has ended) to the external forcing frequency and, at the same time $R(t)$ converges to unity and $\sigma_{\bar{\omega}}(t)$ vanishes.

Notice, furthermore, the non-monotonous behaviour characterising the evolution of $\sigma_{\bar{\omega}}(t)$ (in the second and third columns) as soon as nodes start to be added to $\mathcal{G}_0$. For the three external frequencies reported in Figure 2, indeed, $\sigma_{\bar{\omega}}(t)$ starts from its initial value, increases during the first stage of the growing process, up to reaching a maximum value, and then decreases during the second stage of the growing

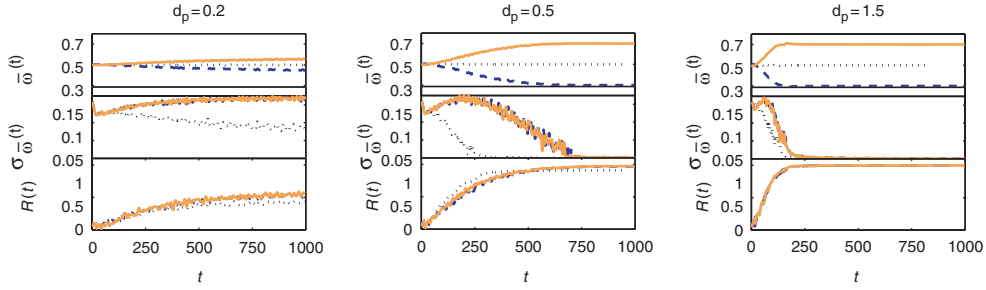

Figure 2. Time evolution of the mean frequency (upper row), frequency dispersion (middle row) and phase synchronisation order parameter (lower row) for three pacemaker frequencies ($\omega_p = 0.7$ orange-solid line, $\omega_p = 0.5$, black-dotted line and $\omega_p = 0.3$ blue-dashed line) and coupling strengths $d_p = 0.2$, 0.5 and 1.5. See text for the definition of all reported quantities. Remaining parameters are as in the caption of Figure 1.

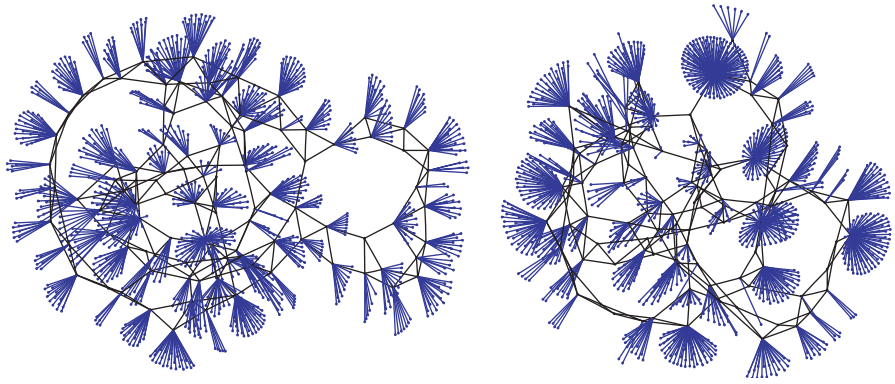

Figure 3. Sketches of two networks constructed for $n_0 = 100$, $n_1 = 1000$ and $\delta = \pi$. The nodes of the original graph are depicted in black, the forcing nodes are depicted in blue. The left(right) network corresponds to a case in which the forcing nodes are unable (able) to entrain $\mathcal{G}_0$ to the pacemaker frequency.

process, eventually saturating to its final value at the end of the growth of the forcing network.

4. The rising of the scale-free network

Once we have showed that the network can be forced by the proposed growing method, let us now focus on the main goal of this study, which is how the degree distribution in $\mathcal{G}_0$ evolves as a result of the phase entrainment process.

As an example, in Figure 3 we show the final graphs obtained for $n_0 = 100$ and $n_1 = 1000$, with the nodes of the original graph (the added nodes) depicted in black (blue). In these plots the very different final structures we obtain can be seen.

The left and right networks correspond to two different outcomes of the growth process: the left network corresponds to the case in which the growing process is unable to entrain $\mathcal{G}_0$ to the pacemaker frequency, and a simple eye inspection shows how the distribution of blue attachments is rather homogeneous. On the other hand, the right graph presents the final structure for a successful entrainment of $\mathcal{G}_0$. Here, one can appreciate the high heterogeneity of the blue attachments, with the simultaneous presence of few nodes with very high degree (hubs), coexisting with a vast majority of nodes featuring comparatively low degrees.

In order to quantify such a difference, we performed extensive simulations of large networks with $n_0 = 1000$, $n_1 = 10{,}000$ and $d_0 = 0.2$, monitoring the time evolution of the degree distribution $P_t(k)$ of the $\mathcal{G}_0$ nodes during the growing process. As we have chosen a small-world topology for $\mathcal{G}_0$, the initial degree distribution $P_0(k)$ peaks around the mean value $\langle k \rangle = k_{0i} = 2m_0$ and has exponentially decaying tails. We here report the *cumulative* degree distribution $P_t^c(k)$, given by $P_t^c(k) = \sum_{k'=k}^{k_{\max}} P_t(k')$, since the summing process of the $P^c(k)$ smooths the fluctuations often observed in the probability of higher degrees.

As a generic property, it is important to remark that if a power-law is observed in the behaviour of $P^c(k)$ (i.e. if $P^c(k) \sim k^{-\gamma_c}$), this also implies that the degree distribution $P(k)$ is characterised by a power-law $P(k) \sim k^{-\gamma}$, with $\gamma \approx 1 + \gamma_c$.

In Figure 4 we show how $P_t^c(k)$ evolves in the two different situations presented in Figure 3. Figure 4(left) depicts the evolution of $P_t^c(k)$ for a failed entrainment. Here it can be seen how the final state of $P_t^c(k)$ deviates significantly from $P_0^c(k)$, but it never approximates to a power-law shape. On the other hand, Figure 4(right) shows the process for a successful entrainment of $\mathcal{G}_0$ to the frequency of the pacemaker. Here, the control process is accompanied by the progressive convergence of $P_t^c(k)$ to a power-law shape.

The difference in the final distributions for the non-entrained and entrained networks, and the convergence in this latter case of $P_t^c(k)$ to a scale-free distribution $P_{\text{end}}^c(k)$ is a generic feature in the parameter space, as can be seen in Figure 5. There, we report log–log plots of $P_{\text{end}}^c(k)$ obtained as the average over 50 different realisations of the growing process for $n_0 = 1000$, $n_1 = 10{,}000$, $d_0 = 0.2$, two different values of δ ($\delta = \pi$ in Figure 5(a),(b) and $\delta = \pi/4$ in Figure 5(c),(d)), two different entrainment frequencies ($\omega_p = 0.5$ in Figure 5(a),(c) and $\omega_p = 0.7$ in Figure 5(b),(d)) and two values of d_p. In all cases, solid (dashed) lines correspond to the entrained (non-entrained) regime, obtained for high (low) values of d_p, and solid red lines indicate the best fits.

Whenever the forcing nodes eventually induce the entrainment of $\mathcal{G}_0$ to the pacemaker frequency, the final degree distribution displays a power-law (scale-free) behaviour $P^c(k) \sim k^{-\gamma_c}$. The specific slope γ_c of the power-law depends on the specific choice of the

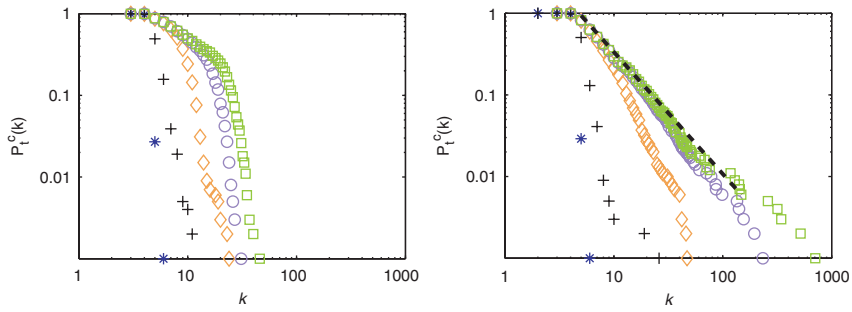

Figure 4. Time evolution of the cumulative degree distribution $P_t^c(k)$ (see text for definition) for a particular realisation of the network growth. $\omega_p = 0.5$ and $d_p = 0.2$ (upper panel, non-entrained graph) and $d_p = 0.5$ (lower panel entrained graph). The time instants at which the distributions are taken are: $t = 0$ (*); $t = 200$ (+); $t = 500$ ($\diamond$); $t = 800$ ($\bigcirc$); $t = 1000$ ($\square$). Notice that, in the entrained case, $P_t^c(k)$ converges to an asymptotic distribution $P_{fin}^c(k)$ ($\square$) which features a power-law shape (best fit sketched with black dashed line).

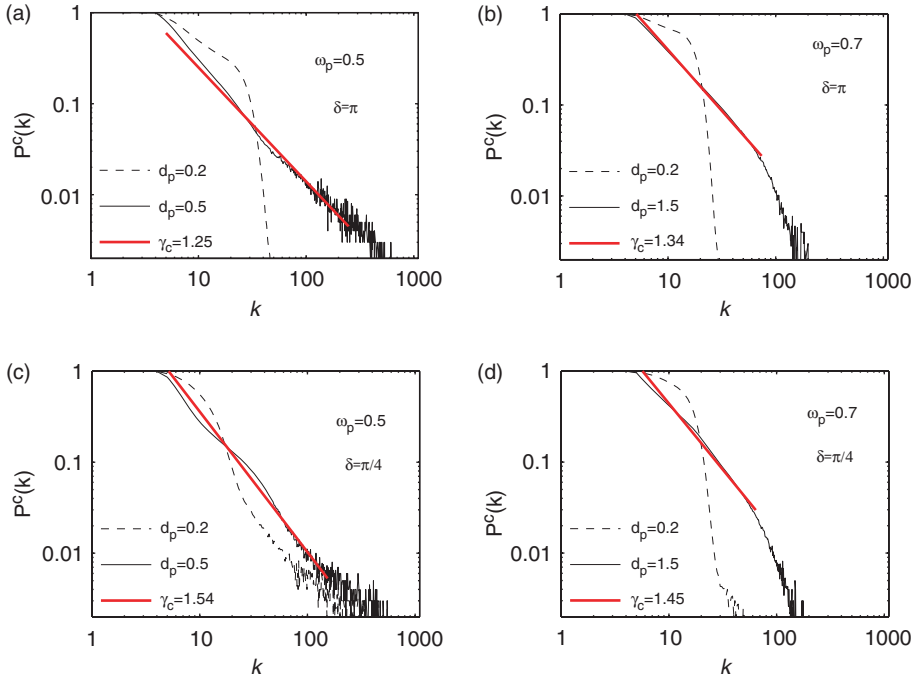

Figure 5. Log-log plots of $P_{\text{end}}^c(k)$ (see text for definition) *vs.* k, averaged over 50 different realisations of the growing process, for: (a)–(b) $\omega_p = 0.5$, 0.7 and $\delta = \pi$, (c)–(d) $\omega = 0.5$, 0.7 and $\delta = \pi/4$. In all cases, solid (dashed) lines correspond to the entrained (non-entrained) regime, obtained for high (low) values of d_p, and solid red lines indicate the best power-law fits. Remaining parameters $n_0 = 1000$, $n_1 = 10{,}000$, $d_0 = 0.2$.

external frequency ω_p. However, in our trials, we always observed values of γ_c in the range $(1, 2)$, in accordance to the values measured for most of the real world networks (Boccaletti et al. 2006b). This is an interesting fact since it is known that the average degree of the network diverges in that case, these values only being possible because the number of connections in the network rapidly increases as it grows.

In order to assure the robustness of the process, we study the possible dependence on diverse changes on the parameters and the initial conditions. In Figure 6 we plot the cumulative degree distribution $P_{\text{end}}^c(k)$ for several choices of the specific initial structure of the pristine network $\mathcal{G}_0$. Here it can be seen that in all cases the growing process leads to the same qualitative scenario, showing a power-law distribution with the same γ_c. Additionally, although they are not shown here for avoiding repetition, the results reported have also been checked to be qualitatively independent on both the system size and the value of $\delta \in (0, 2\pi)$. We have also considered the

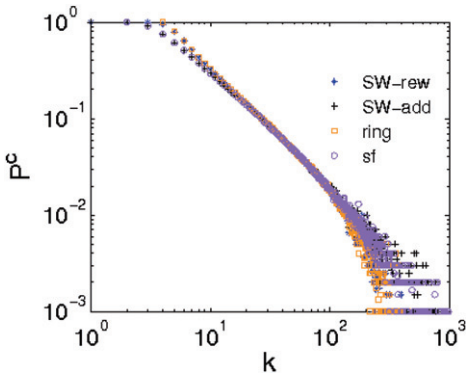

Figure 6. Cumulative degree distribution $P^c_{\text{end}}(k)$ for several choices of the original wiring of the pristine network $\mathcal{G}_0$: small-world with rewiring (SW-rew), small-world with adding (SW-add), ring and scale-free (sf).

case in which each new added node has m > 1 links. In this condition, as expected, the process becomes faster, in the sense that the number of new nodes needed to entrain the network reduces, but the final topology has the same properties as that for the previously studied case $m = 1$. Therefore, we conclude that the observed scenario is generic for a wide range of conditions.

5. Discussion and conclusions

The relationship between the entrainment process and the rising of a scale-free degree distribution can be interpreted as follows. Each oscillator in the original graph $\mathcal{G}_0$ can be found in two different states with respect to the pacemaker: the phase locked state, and the phase untrained state. When an oscillator is in the phase untrained state, its phase difference with respect to that of the pacemaker can be represented as a point in the unit circle that is circulating clockwise or counterclockwise, depending on whether the difference between the frequency of the oscillator and that of the pacemaker is positive or negative. When, instead, the oscillator is in the phase locked state, the dynamics of the phase difference $\Delta\theta$ is locked around the value $\Delta\theta = 0$, as this latter represents the fixed point corresponding to phase entrainment.

In practice, this means that, during the growing process, if a given node entrains its phase to that of the pacemaker at a given time, it is prevented from receiving further attachments coming from future nodes. This is because we explicitly select the phase condition to be different from zero, and therefore the entrained node (whose phase difference will henceforth stay around the fixed point) will never again satisfy the condition needed to get further attachments. All the other untrained nodes will continue rotating and therefore at least one of them will always better satisfy the required phase difference condition with the attachment.

Let us try to describe the entire scenario that is actually observed by starting from a network $\mathcal{G}_0$ composed of n_0 unsynchronised nodes. As initially all the nodes are unsynchronised, the very first connection just selects the network element whose phase is occasionally the closest to the given δ at that given moment of time. Therefore, each of the nodes will have $1/n_0$ probability of acquiring the first connection. If the value of d_p associated to each connection is low, insufficient to produce phase entrainment of the nodes, only the very few nodes whose original frequency was close to that of the pacemaker will be able to entrain their phases at that value of d_p, but the vast majority of nodes, though perturbed in their phase dynamics, will never be able to entrain their phases. As a result, apart from those very few nodes, there will be always a set of $N_{\text{untrained}} \sim n_0$ nodes that can acquire further connections with equal probability, and therefore the process is effectively resembling a random shooting. This is the reason why the observed variation in the degree distribution never leads to a scale-free behaviour (it is well known that any random attachment assuming uniform probability gives degree distributions with exponential, and not power-law, tails), as in the example in the left panel of Figure 4 .

Instead, large values of d_p are able to entrain all nodes to the frequency of the pacemaker, independently on their initial frequency. Here again, initially, all nodes will have $1/n_0$ probability of acquiring the first connection. However, as soon as the first node is trained, the remaining nodes have $1/(n_0 - 1)$ probability of acquiring a further connection. Then, in general, any state has S nodes already trained and $n_0 - S$ nodes still untrained; these last ones have $1/(n_0 - S)$ probability of acquiring a further connection. Therefore, the issue is now which nodes are the first ones to get the trained state. Here again, as initially all nodes have the same probability of getting a connection, it is reasonable to assume that the first nodes to get the trained state will be those with original frequency closer to the pacemaker (those, e.g. for which the needed perturbation to be entrained is smaller, and therefore those for which just a few added connections are yet able to determine their phase entrainment). As a result, it should be expected that the nodes originally displaying a larger frequency mismatch will increase (in course of time) their probability of getting further connections during the growing process. This is equivalent to saying that the present process gives rise to a sort of preferential attachment where the final hubs will be those nodes for which the absolute value

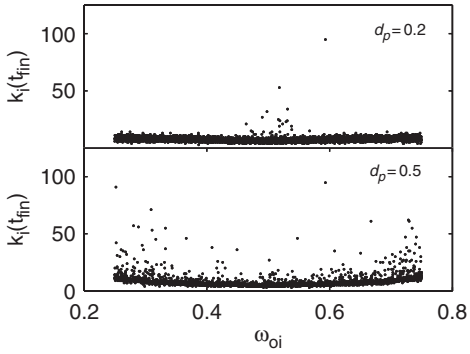

Figure 7. Final number of connections $k_i(t_{\text{fin}})$ acquired by each node as a function of its initial frequency ω_{0i} for $\omega_p = 0.5$, $\delta = \pi$, and $d_p = 0.2$ (upper plot, untrained case) and $d_p = 0.5$ (lower plot, trained case).

of the frequency mismatch is higher, as is the case of the right panel in Figure 4.

This qualitative scenario is confirmed in Figure 7, where we report the final number of acquired connections $k_i(t_{\text{fin}})$ for each node as a function of the original frequency ω_{0i} for a frequency of the pacemaker $\omega_p = 0.5$ and for two values of d_p. It can be noted that $k_i(t_{\text{fin}})$ is nothing but proportional to the probability of the i-th node to acquire a connection during the entire growing process, as this latter quantity can be obviously written as the total number of connections received by the i-th node divided by the total number of shootings. Figure 7 shows that in the untrained case ($d_p = 0.2$), the distribution is almost uniform, reflecting a random shooting which gives rise to a non-scale-free degree distribution, while in the trained case ($d_p = 0.5$), the nodes whose original frequency mismatch was higher have a clearly higher probability to get connections as a result of the growing process.

We point out that the situation is slightly complicated by the fact that the growing mechanism starts (as detailed in the text) after a first evolution of $\mathcal{G}_0$, where the distribution of frequencies of the oscillators is slightly rearranged. This results in the presence of some nodes of high degree near to the frequency of the pacemaker, see lower plot of Figure 7. Those points correspond to oscillators whose initial frequencies were, indeed, close to that of the pacemaker, but whose instantaneous frequencies at the instant at which the growing process starts were moved away from that of the pacemaker by the initial rearrangement.

Additional questions can be considered for future research. It will be important to know how robust is the system to the presence of noise, which perhaps could affect the final topology. In addition, other node dynamics and criteria should be considered, as synchronisation for excitable nodes. The extension of the study to stochastic systems or the inclusion of time delays should also be explored (Wang, Shu, Fang, and Liu 2006a; Wang, Liu, Li, and Liu 2006b).

In summary, we have shown how a phase-entrainment growing process entirely guided by dynamical criteria is able to fully reshape the topology of the original network, and that the entrainment process is associated with the emergence of a scale-free degree distribution in the graph connectivity. This fact can therefore give new hints on the fundamental processes that rule the growth of some of the real world networks, which ubiquitously feature such kind of connectivity distributions.

Acknowledgements

Authors acknowledge Maya Paczuski for valuable comments. This work was partly supported by the Spanish Ministry of Science and Technology under Project No. FIS2006-08525 and the URJC-CM Projects Nos. PPR2004-04 and URJC-CM-2007-CET-1602.

References

Barabási, A.L., and Albert, R. (1999), 'Emergence of Scaling in Random Networks', *Science*, 286, 509–512.

Boccaletti, S., Hwang, D., Chavez, M., Amann, A., Kurths, J., and Pecora, L.M. (2006a), 'Synchronization in Dynamical Networks: Evolution along Commutative Graphs', *Physical Review E*, 74, 016102.

Boccaletti, S., Latora, V., Moreno, Y., Chavez, M., and Hwang, D.U. (2006b), 'Complex Networks: Structure and Dynamics', *Physics Report*, 424, 509.

Chavez, M., Hwang, D.U., Amann, A., Hentschel, H., and Boccaleti, S. (2005a), 'Synchronization is Enhanced in Weighted Complex Networks', *Physical Review Letters*, 94, 218701.

Chavez, M., Hwang, D.U., Amann, A., Hentschel, H., and Boccaletti, S. (2005b), 'Synchronization in Complex Networks with Age Ordering', *Physical Review Letters*, 94, 138701.

Ebel, H., and Bornholdt, S. (2002), Evolutionary Games and the Emergence of Complex Networks, eprint cond-mat/0211666.

Kuramoto, Y. (1984), *Chemical Oscillations, Waves, and Turbulence*, Berlin: Springer.

Motter, A.E., Zhou, C., and Kurths, J. (2005), 'Network Synchronization, Diffusion, and the Paradox of Heterogeneity', *Physical Review E*, 71, 016116.

Sendiña-Nadal, I., Buldú, J.M., Leyva, I., and Boccaletti, S. (2008), 'Phase Entrainment Induces Scale-Free Topologies in Networks of Coupled Oscillators', *PLoS ONE*, 3, e2644.

Stilwell, D.J., Bollt, E.M., and Roberson, D.G. (2006), 'Sufficient Conditions for Fast Switching Synchronization

in Time-Varying Network Topologies', *SiAM Journal on Applied Dynamical Systems*, 5, 140.

Strogatz, S. (2000), 'From Kuramoto to Crawford: Exploring the Onset of Synchronization in Populations of Coupled Oscillators', *Physica D*, 143, 1.

Yin, C.Y., Wang, W.X., Chen, G., and Wang, B.H. (2006), 'Decoupling Process for Better Synchronizability on Scale-Free Networks', *Physical Review E*, 74, 047102.

Wang, Z., Shu, H., Fang, J., and Liu, X. (2006a), 'Robust Stability for Stochastic Hopfield Neural Networks with Time Delays', *Nonlinear Analysis: Real World Applications*, 7, 1119.

Wang, Z., Liu, Y., Li, M., and Liu, X. (2006b), 'Stability Analysis for Stochastic Cohen-Grossberg Neural Networks with Mixed Time Delays', *IEEE Transactions on Neural Networks*, 17, 814.

Zimmermann, M.G., Eguíluz, V.M., and Miguel, M.S. (2004), 'Coevolution of Dynamical States and Interactions in Dynamic Networks', *Physical Review E*, 69, 065102(R).